CrossMark

ORIGINAL PAPER

Comparison of monthly rainfall generated from dynamical and statistical downscaling methods: a case study of the Heihe River Basin in China

Haifeng Su[1,2] · Zhe Xiong[1] · Xiaodong Yan[3] · Xingang Dai[1] · Wenguang Wei[1,2]

Abstract Monthly rainfall in the Heihe River Basin (HRB) was simulated by the dynamical downscaling model (DDM) and statistical downscaling model (SDM). The rainy-season rainfall in the HRB obtained by SDM and DDM was compared with the observed datasets (OBS) over the period of 2003–2012. The results showed the following: (1) Both methods reasonably reproduced the spatial pattern of rainy-season rainfall in the HRB with a high-level skill. Rainfall simulated by DDM was better than that by SDM in the upstream, with biases of −12.09 and −13.59 %, respectively; rainfall simulated by SDM was better than that by DDM in the midstream, with biases of 3.91 and −23.22 %, respectively; there was little difference between the rainfall simulated by SDM and DDM in the downstream, with biases of −10.89 and −9.50 %, respectively. (2) Both methods reasonably reproduced monthly rainfall in rainy season in different subregions. Rainfall simulated by DDM was better than that by SDM in May and July in the upstream, whereas rainfall simulated by SDM was closer to OBS except August in the midstream and except August and September in the downstream. (3) For multi-year mean rainy-season rainfall in different stations, there was a little difference between the rainfall simulated by DDM and SDM in Tuole station in the upstream, with

biases of −13.16 and −12.40 %, respectively; rainfall in Zhangye station simulated by SDM was overestimated with bias of 14.02 %, and rainfall simulated by DDM was underestimated with bias of −14.60 %; rainfall in Dingxin station simulated by DDM was reproduced better than that by SDM, with biases of −19.34 and −32.75 %, respectively.

1 Introduction

Northwest China accounts for one third of the territory, but only 5 % of the water resources of China. Water shortage is one of the most important factors that restrict the economic development and ecological deterioration for the Northwest region. In the background of global climate continuing to warm, the tendency of water resources in the Northwest arid area of China must be carefully considered by the strategy formulation for regional economy development and the management of water resources and also attracts high attention of research community (Lan et al. 2005). The Heihe River Basin (HRB) is the second largest inland river basin in Northwest China, which is located in 98–101.5° E, 38–42° N, with the drainage area of about 130 km² and a total length of about 810 km. The land type of HRB can be divided into three categories: mountain, oasis, and desert (Cheng et al. 2006). Water resources are the core of the Heihe River research and the link of ecological and economic system. Rainfall is one of the most important parameters of the hydrological system and the main sources of water resources in the HRB. Therefore, the rainfall data with high spatial resolution has important guiding significance on the sustainable development of society, economy and environment, and the hydrological research in Northwest China. Global climate models (GCMs) or reanalysis data could be used to simulate rainfall scenarios. However, GCMs are not able to provide reliable information

✉ Zhe Xiong
  xzh@tea.ac.cn

1   Key Laboratory of Regional Climate–Environment for Temperate
     East Asia, Institute of Atmospheric Physics, Chinese Academy of
     Sciences, NO. 40 HuaYanLi, Beijing, ChaoYang District 100029,
     China

2   University of Chinese Academy of Sciences, Beijing 100049, China

3   State Key Laboratory of Earth Surface Processes and Resource
     Ecology, Beijing Normal University, Beijing 100087, China

on a regional scale. At the same time, the spatial distribution of ground observations is uneven and sparse, with only 19 meteorological stations in the HRB region. Hence, downscaling methods could be applied to compensate for these deficiencies (Gao et al. 2008).

Downscaling techniques are often used to derive high spatial resolution rainfall datasets from GCMs or reanalysis data, which can be broadly divided into two approaches: dynamical downscaling (e.g., Druyan et al. 2002; Lenderink et al. 2007; Denis et al. 2002) and statistical downscaling (e.g., Wilby et al. 1997, 2000; von Storch et al. 1993; Maraun et al. 2011). Dynamical downscaling uses GCMs or reanalysis data as boundary and initial conditions to drive a regional climate model (RCM), which includes numerous physical processes and does not depend on observations. Numerous dynamical downscaling models have been used to simulate rainfall in the USA (e.g., Harding et al. 2014), West Africa (e.g., Siegmund et al. 2014), Southwest Asia (e.g., Xu et al. 2012), and Europe (e.g., Murphy, 1999; Schmidli et al. 2007). In the HRB, some RCMs were applied to predict regional climate change (e.g., Pan et al. 2012; Gao et al. 2006, 2007; Liu et al. 2008). However, these RCMs adopted international standard parameters without considering the effects of the complex terrain and surface features (Xiong et al. 2013).

Statistical downscaling establishes statistical relationships between large-scale GCMs or reanalysis data (predictors) and local-scale meteorological variables (predictands) and extends these relationships to obtain the time series of predictands from the predictors. Numerous statistical downscaling methods have been applied to simulate rainfall in many regions. Storch et al. (1993) used canonical correlation analysis (CCA) to construct a simple statistical regression model to simulate wintertime rainfall of the Iberian Peninsula in Europe. The analog method was used to simulate rainfall in the USA (Zorita et al., 1994). Principal component regression models were used to simulate winter rainfall in Southern Australia (Li et al. 2008). However, the statistical downscaling technique has not been applied to the study of hydrological cycle in the HRB with scarcely and unevenly meteorological observations.

There have been numerous studies to compare the skill of simulating rainfall in many regions by statistical and dynamical downscaling methods (e.g., Murphy 1999; Mearns et al. 1999; Mehrotra et al., 2014). Furthermore, the period of rainfall in the HRB is mainly concentrated in the rainy season (from May to September) (Zhang et al., 2008). Therefore, in the paper, a dynamical downscaling model (DDM) with a high resolution of 3 km was build up based on the Regional Integrated Environmental Model System (RIEMS 2.0). The observed monthly rainfall in the HRB (predictands) and 14 reanalysis variables (predictors) were used to establish a statistical downscaling model (SDM) by the stepwise regression method. Monthly rainfall in rainy season in the HRB over the

period of 2003–2012 was simulated by SDM and DDM to compare with the observed datasets (OBS). The main goals are to systematically compare the capability of simulating monthly rainfall and explore the advantages and disadvantages of the two downscaling models in the HRB.

2 Data and methods

2.1 Data

2.1.1 Observation stations datasets

Monthly rainfall of 10 meteorological observation stations selected from 19 stations, which include with missing values, are used as predictands to fit the statistical model (Fig 1, Table 1). The data from 1971 to 2012 is obtained from the Chinese Meteorological Data Sharing Service System (http://cdc.cma.gov.cn).

2.1.2 Predictors selection

In the study, sea level pressure (SLP), wind speed, and direction at 850, 700, and 500 hPa (U/V850, U/V700, U/V500), geopotential height at 1000, 850, 700, and 500 hPa (H1000, H850, H700, H500), and specific humidity at 850, 700, and 500 hPa (S850, S700, S500) are selected as predictors according to Wetterhall et al. (2006). These 14 predictors with resolution of $2.5° \times 2.5°$ are obtained from the National Center for Environmental Prediction/National Center for Atmospheric Research (NCEP/NCAR) reanalysis project (Kalnay et al. 1996).

## 2.2 Statistical downscaling model

Firstly, monthly rainfall over the period of 1971–2002 as training sample is used to establish the statistical model. The predictors and predictands are standardized as follows:

$$Y = (X - b)/c, \quad (1)$$

where Y is the standard value; X is a predictor (SLP, U/V850, U/V700, U/V500, H1000, H850, H700, H500, S850, S700, or S500) or a predictand (monthly rainfall); b is the mean monthly value of X; and c is the standard deviation of X.

Then, principal component analysis (PCA) to these 14 predictors is applied. The general aim of PCA is to simplify a spatial–temporal dataset by transforming it to spatial patterns of variability and temporal projections of these patterns. The associated temporal projections are the principal components (PCs) and are the temporal coefficients of the empirical orthogonal function (EOF) patterns. PCA helps to reduce the numbers of variables in a dataset without losing much of the information. This objective method can be achieved by including only the first

Fig. 1 Spatial distribution of meteorological stations in the HRB
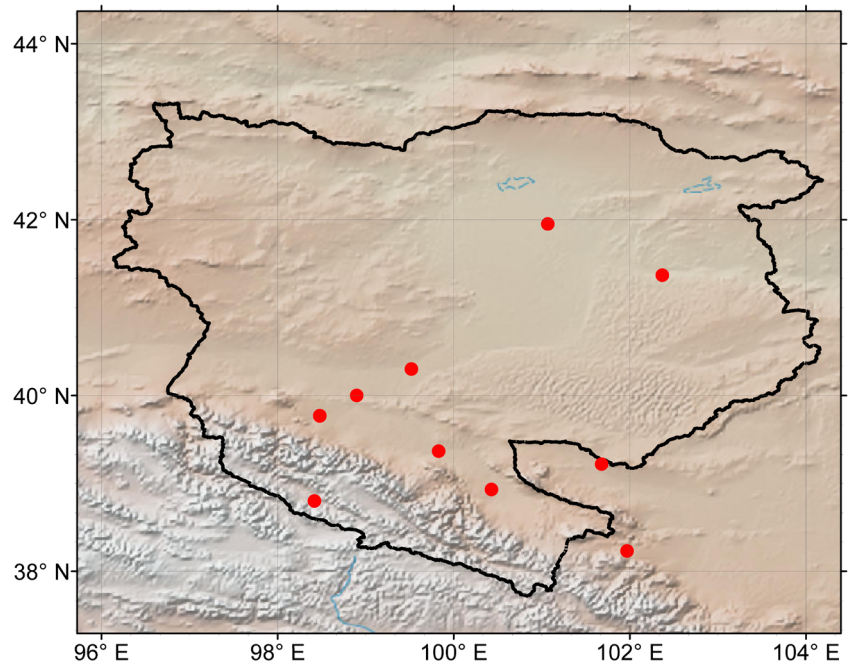
few PCs (Ruping et al., 2002). Therefore, the first four PCs of every predictor were selected to establish statistical models.

Last, stepwise regression method is used to develop the model as follows:

$$Y(t) = \sum_{n=1}^{N} \alpha_n X_n(t) + \varepsilon_t , (2).$$

where Y is the predictand (monthly rainfall), X is the predict variable ($N = 56$), α is the regression coefficient, and ε_t is the residual not described by the statistical model.

For simplicity, only the selected predictors for the month of July at 10 stations are shown in Table 2. It can be seen that S700 and S850 are the most important predictors for rainfall in the HRB.

2.3 Dynamical downscaling model

The high-resolution RCM for HRB was built up. The key parameter datasets of land surface process provided by the Environmental and Ecological Science Data Center for West China, National Natural Science Foundation of China, which included the soil water content, soil water potential, soil hydraulic conductivity, field capacity, and wilt point moisture content, were recalibrated (Xiong et al. 2013). Initial and lateral boundary conditions for wind, temperature, water vapor, and surface pressure were extracted from ERA–interim reanalysis data (Dee et al., 2011), which was downloaded from the European Center for Medium Range Weather Forecasts Data Server. The simulated domain encompassed the entire HRB region, centered at 40.30° N, 99.50° E; the horizontal

Table 1 Coordinates and altitudes of stations

Station	NO.	Longitude (°N)	Latitude (°E)	Altitude (m)
Ejinaqi	52,267	101.07	41.95	940.5
Guaizihu	52,378	102.37	41.37	960.0
Dingxin	52,446	99.52	40.30	1177.4
Jinta	52,447	98.90	40.00	1270.5
Jiuquan	52,533	98.48	39.77	1477.2
Gaotai	52,546	99.83	39.37	1332.2
Alashanyouqi	52,576	101.68	39.22	1510.1
Tuole	52,633	98.42	38.80	3367.0
Zhangye	52,652	100.43	38.93	1482.7
Yongchang	52,674	101.97	38.23	1976.9

Table 2 Variables were selected for the month of July at 10 stations

NO.	July
1	V500(2), S850(1), H500(4)
2	S850(1), V500(2), V700(2)
3	V50(2), S700(1), U500(2), H700(3)
4	S700(1), U500(2), H500(2)
5	V850(2), S700(4), S700(1), H850(3)
6	S850(3), S850(1), V500(3), SLP(2)
7	H500(2), U850(2), S850(1)
8	H850(3), S700(1), H500(2), S700(4)
9	S700(1), U850(2), V500(2), U500(2), H500(1)
10	S850(1), U850(2)

The numbers (1)–(4) represent 1–4 PC of every predictor, respectively

mesh consisted of 181 and 221 grid points in the longitudinal and latitudinal directions, respectively, with a horizontal resolution of 3 km. The high-resolution RCM have finished simulating the rainfall in the HRB for the period from January, 2003 to December, 2012 (Xiong et al. 2013).

3 Results

3.1 Spatial distribution of rainy-season rainfall

The annual rainfall in the HRB is 400–700 mm in the upstream at Qilian Mountain, 100–200 mm in the midstream at the irrigated oases, and 15–50 mm in the downstream at the desert. The HRB is divided into three subregions according to the characteristics of rainfall: upstream (Yongchang and Tuole stations), midstream (Gaotai, Alashanyouqi, Jiuquan, and Zhangye stations), and downstream (Dingxin, Jinta, Ejinaqi, and Guaizihu stations) (Cheng et al. 2006).

Rainy-season rainfall in three subregions over the period of 2003–2012 is simulated by SDM and DDM. From Table 3, it can be seen that the observed rainfall in the upstream is 249.38 mm. Rainfall simulated by SDM is 219.25 mm with bias of −12.09 %, and RMSE and mean absolute error (MAE) between SDM and OBS are 41.30 and 33.26 mm, respectively; whereas rainfall simulated by DDM is 225.92 mm with bias of −9.42 %, and RMSE and MAE between DDM and OBS are 42.09 and 35.52 mm, respectively. Rainfall simulated by DDM is better than that by SDM in the upstream.

The observed rainfall in the midstream is 95.61 mm. Rainfall simulated by SDM is 99.35 mm with bias of 3.91 %, and RMSE and MAE between SDM and OBS are 20.14 and 18.10 mm, respectively; whereas rainfall simulated by DDM is 73.42 mm with bias of −23.22 %, and RMSE and MAE between DDM and OBS are 37.74 and 32.78 mm, respectively. Rainfall simulated by SDM is better than that by DDM in the midstream.

The observed rainfall in the downstream is 43.49 mm. Rainfall simulated by SDM is 38.75 mm with bias of −10.89 %, and RMSE and MAE between SDM and OBS are 14.44 and 12.60 mm, respectively; whereas rainfall simulated by DDM is 39.36 mm with bias of −9.50 %, and RMSE and MAE between DDM and OBS are 12.29 and 9.87 mm,

respectively. There was a little difference between the rainfall simulated by SDM and DDM in the downstream.

In general, both methods reasonably reproduced the rainy-season rainfall in the HRB with a high-level skill. Rainfall simulated by DDM is better than that by SDM in the upstream, with biases of −12.09 and −13.59 %, respectively; rainfall simulated by SDM is better than that by DDM in the midstream, with biases of 3.91 and −23.22 %, respectively; there is little difference between the rainfall simulated by SDM and DDM in the downstream, with biases of −10.89 and −9.50 %, respectively. Both methods have their own advantages.

Figure 2 is the time series of rainy-season rainfall. The observed rainfall in the upstream is in the range of 1.40–1.98 mm/day. Rainfall simulated by SDM is in the range of 1.19–1.63 mm/day with maximal bias of −28.64 % in 2011; whereas rainfall simulated by DDM is in the range of 1.07–1.92 mm/day with maximal bias of −32.20 % in 2003.

The observed rainfall in the midstream is in the range of 0.46–0.82 mm/day. Rainfall simulated by SDM is in the range of 0.48–0.79 mm/day, all of biases are in the range of −50–50 %; whereas rainfall simulated by DDM is in the range of 0.19–0.75 mm/day, which gives biases larger than 50 % in 2003–2005 and 2011.

The observed rainfall in the downstream is in the range of 0.18–0.41 mm/day. The rainfall simulated by SDM is in the range of 0.13–0.38 mm/day, which gives positive biases larger than 50 % in 2006; whereas rainfall simulated by DDM is in the range of 0.12–0.53 mm/day with bias of −38.95–36.04 %.

In general, most biases of two models are in the range of −50–50 %, which are consistent with the IPCC TAR (Houghton et al. 2001); thus, both SDM and DDM well simulate the time series of rainy-season rainfall in the HRB.

3.2 Monthly rainfall in rainy–season

Figure 3 shows monthly rainfall in the HRB. From Fig. 3, it can be seen that the observed rainfall in the upstream is in the range of 0.94 (May)–2.50 (July) mm/day. Rainfall simulated by SDM is in the range of 0.81 (May)–2.06 (July) mm/day with biases of −19.87–1.84 %; whereas rainfall simulated by DDM is in the range of 1.00 (May)–2.17 (July) mm/day with

Table 3 OBS and rainy-season rainfall simulated by SDM and DDM, bias, and RMSE and MAE between OBS and two models in the subregions of HRB

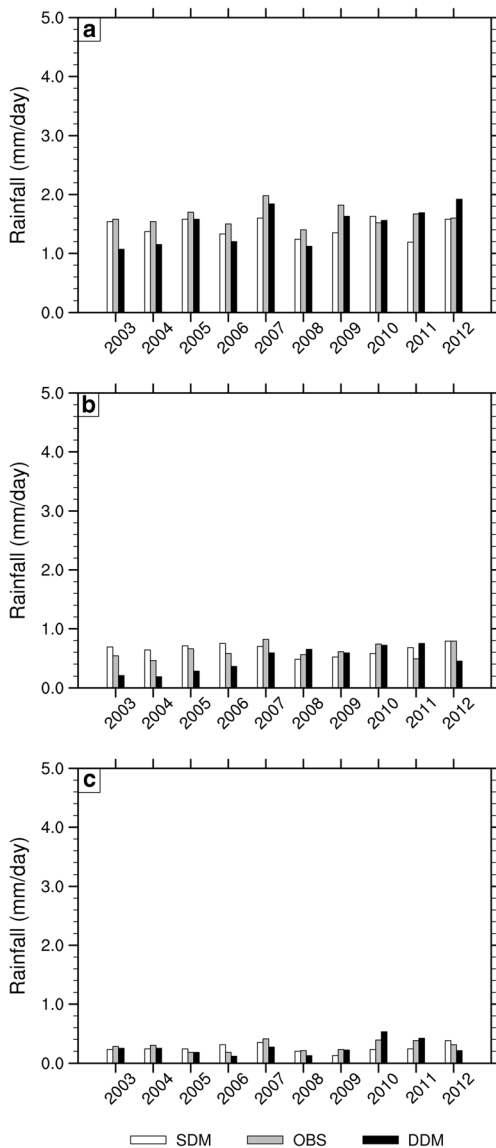|		Statistical downscaling model				Dynamical downscaling model			
	OBS (mm)	SDM (mm)	Bias (%)	RMSE (mm)	MAE (mm)	DDM (mm)	Bias (%)	RMSE (mm)	MAE (mm)
Upper	249.38	219.25	−12.09	41.30	33.26	225.92	−9.42	42.09	35.52
Middle	95.61	99.35	3.91	20.14	18.10	73.42	−23.22	37.74	32.78
Lower	43.49	38.75	−10.89	14.44	12.60	39.36	−9.50	12.29	9.87

Fig. 2 The time series of rainy-season rainfall (mm/day) in the subregions of HRB: **a** upstream, **b** midstream, and **c** downstream

the range of 0.07 (May)–0.43 (September) mm/day with biases of −47.43–33.29 %. For a different month, rainfall simulated by SDM is closer to OBS than that by DDM except August and September.

In general, most biases of monthly rainfall simulated by SDM and DDM are in the range of −50–50 %, which are consistent with the IPCC TAR. Therefore, both methods reasonably reproduce the monthly rainfall in rainy–season in different subregions. Rainfall simulated by DDM is better than that by SDM in May and July in the upstream; whereas rainfall simulated by SDM is closer to OBS except August in the midstream and except August and September in the downstream. In addition, the maximal and minimal values of OBS in three subregions are in July and May, respectively. However, DDM cannot capture this pattern in the midstream and downstream.
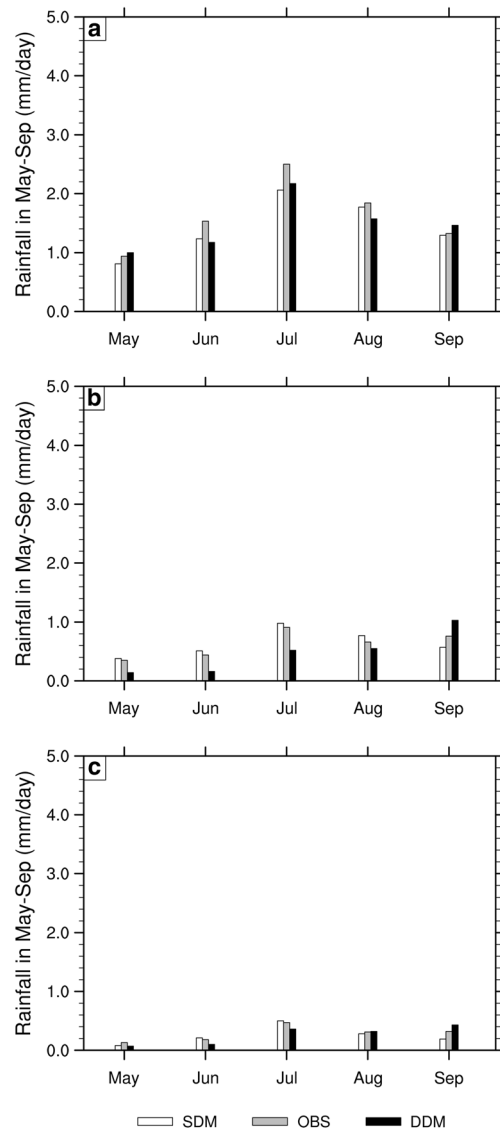

Fig. 3 Monthly rainfall (mm/day) in rainy-season in the subregions of HRB: **a** upstream, **b** midstream, and **c** downstream

biases of −23.67–11.03 %. For different month, rainfall simulated by DDM is better than that by SDM in May and July.

The observed rainfall in the midstream is in the range of 0.35 (May)–0.91 (July) mm/day. Rainfall simulated by SDM is in the range of 0.38 (May)–0.98 (July) mm/day with biases of −24.78–15.65 %; whereas rainfall simulated by DDM is in the range of 0.14 (May)–1.03 (September) mm/day and tends to monthly increase with biases of −63.81–35.62 %, which gives negative biases larger than 50 % in May and June. For a different month, rainfall simulated by SDM is close to OBS than that by DDM except August.

The observed rainfall in the downstream is in the range of 0.13 (May)–0.47 (July) mm/day. Rainfall simulated by SDM is in the range of 0.08 (May)–0.50 (July) mm/day with biases of −41.54–15.30 %; whereas rainfall simulated by DDM is in

3.3 Comparison with stations

Tuole meteorological observation station, a typical station in the upstream, is located in 98.42° N, 38.80° E. The average annual rainfall is more than 300 mm over the period of 1971–2012. Figure 4 shows the rainfall obtained by SDM and DDM are compared with the OBS in July. The correlation coefficient between DDM and OBS is 0.43 and reaches a significance level of 1 %, and it is 0.23 between SDM and OBS.

Figure 5 shows the monthly rainfall in rainy season in Tuole, Zhangye, and Dingxin station. The observed rainfall in Tuole station in the upstream is in the range of 1.13 (May)–3.33 (July) mm/day. Rainfall simulated by SDM is in the range of 1.00 (May)–2.56 (July) mm/day with biases of −32.56–13.96 %; whereas rainfall simulated by DDM is in the range of 0.80 (September)–3.13 (July) mm/day with biases of −38.72–3.54 %. Biases of DDM are minor than that of SDM in May, June, and July.

The observed rainfall in Zhangye station in the midstream is in the range of 0.50 (May)–0.93 (September) mm/day. Rainfall simulated by SDM is in the range of 0.36 (May)–1.27 (September) mm/day with biases of −28.39–44.87 %; whereas rainfall simulated by DDM is in the range of 0.18 (May)–1.19 (September) mm/day with biases of −64.18–27.43 %, which gives significant underestimates in May and June with biases larger than 50 %. Furthermore, similar to the midstream, rainfall in Zhangye station simulated by DDM tends to monthly increase. Biases of SDM are minor than that of DDM in May, June, and September.

The observed rainfall in Dingxin station in the downstream is in the range of 0.12 (May)–0.58 (July) mm/day. Rainfall simulated by SDM in the range of 0.05 (May)–0.58 (July) mm/day with biases of −63.79–0.04 %, which gives biases larger than 50 % in May and August; whereas rainfall simulated by DDM is in the range of 0.08 (June)–0.54 (September) mm/day with biases of −68.59–40.23 %, which gives a underestimate with bias larger than 50 % in June. Biases of DDM are minor than that of SDM in May, August, and September.

The multi-year average rainy-season rainfall in three stations is listed in Table 4. The observed rainfall in Tuole station
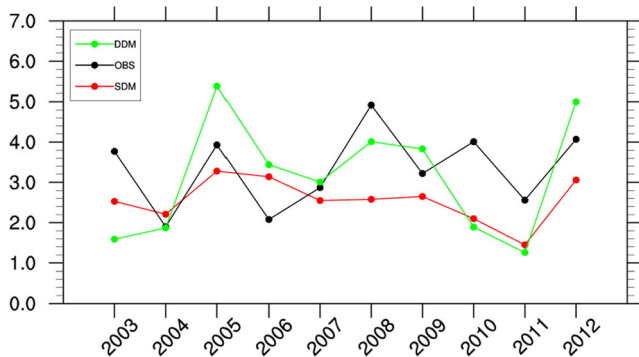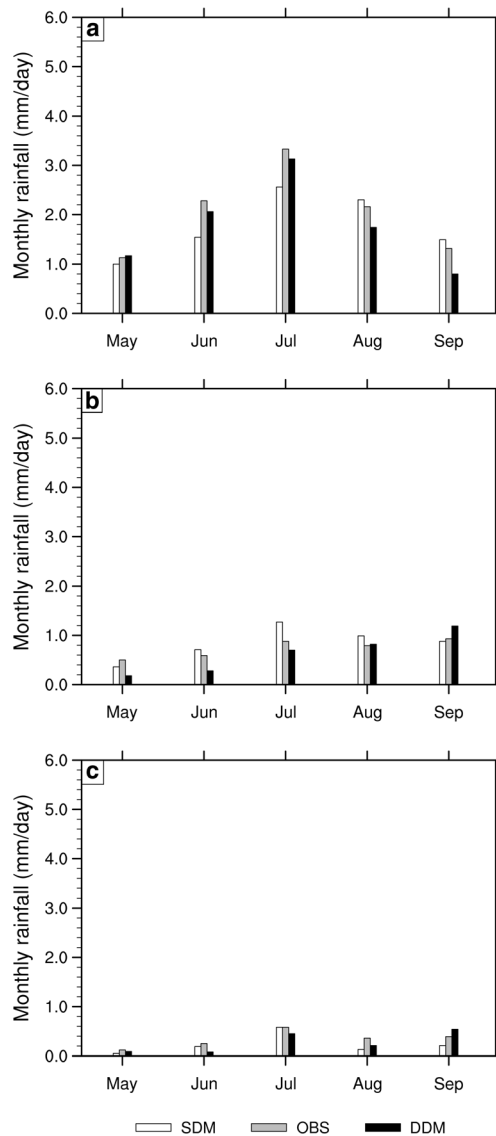

Fig. 4 Rainfall (mm/day) in July in Tuole station

Fig. 5 Monthly rainfall (mm/day) in **a** Tuole station, **b** Zhangye station, and **c** Dingxin station

is 313.85 mm. Rainfall simulated by SDM is 272.55 mm with bias of −13.16 %, and RMSE and MAE between SDM and OBS are 56.41 and 43.01 mm, respectively; whereas rainfall simulated by DDM is 274.94 mm with bias of −12.40 %, and RMSE and MAE between DDM and OBS are 59.42 mm and 44.01 mm, respectively. There was a little difference between the rainfall simulated by DDM and SDM.

The observed rainfall in Zhangye station is 113.19 mm. Rainfall simulated by SDM is 129.06 mm with bias of 14.02 %, and RMSE and MAE between SDM and OBS are 37.31 and 30.54 mm, respectively; whereas rainfall simulated by DDM is 96.70 mm with bias of −14.60 %, and RMSE and MAE between DDM and OBS are 46.08 and 37.82 mm, respectively.

The observed rainfall in Dingxin station is 52.97 mm. Rainfall simulated by SDM is 35.62 mm with bias of

Table 4 OBS and rainy-season rainfall simulated by SDM and DDM, bias, and RMSE and MAE between OBS and two models in three stations

Station	OBS (mm)	Statistical downscaling model				Dynamical downscaling model			
		SDM (mm)	Bias (%)	RMSE (mm)	MAE (mm)	DDM (mm)	Bias (%)	RMSE (mm)	MAE (mm)
Tuole	313.85	272.55	−13.16	56.41	43.01	274.94	−12.40	59.42	44.01
Zhangye	113.19	129.06	14.02	37.31	30.54	96.70	−14.60	46.08	37.82
Dingxin	52.97	35.62	−32.75	26.08	22.21	41.92	−19.34	25.24	20.72

−32.75 %, RMSE and MAE between SDM and OBS are 26.08 and 22.21 mm, respectively; whereas rainfall simulated by DDM is 41.92 mm with bias of −19.34 %. RMSE and MAE between DDM and OBS are and 25.24 and 20.72 mm, respectively. Rainfall simulated by DDM is reproduced better than that by SDM in Dingxin station.

In general, for multi-year mean rainy-season rainfall in different stations, there is a little difference between the rainfall simulated by DDM and SDM in Tuole station in the upstream, with biases of −13.16 and −12.40 %, respectively; rainfall in Zhangye station simulated by SDM is overestimated with bias of 14.02 %, and rainfall simulated by DDM is underestimated with bias of −14.60 %; rainfall in Dingxin station simulated by DDM is reproduced better than that by SDM, with biases of −32.75 and −19.34 %, respectively. For a different month, biases of DDM are minor than that of SDM in May, June, and July in Tuole station, and in May, August, and September in Dingxin station; whereas biases of SDM are minor than that of DDM in May, June, and September in Zhangye station.

4 Discussion and conclusion

Statistical and dynamical downscaling methods simulated monthly rainfall of rainy season in three subregions of the HRB. The results showed the following: (1) Both methods reasonably reproduced the spatial pattern of rainy-season rainfall in the HRB with a high-level skill. Rainfall simulated by DDM was better than that by SDM in the upstream, with biases of −12.09 and −13.59 %, respectively; rainfall simulated by SDM was better than that by DDM in the midstream, with biases of 3.91 and −23.22 %, respectively; there was a little difference between the rainfall simulated by SDM and DDM in the downstream, with biases of −10.89 and −9.50 %, respectively. For a different month, rainfall simulated by DDM was better than that by SDM in May and July in the upstream, whereas rainfall simulated by SDM was closer to OBS except August in the midstream and except August and September in the downstream. (2) For multi-year mean rainy-season rainfall in different stations, there was little difference between the rainfall simulated by DDM and SDM in Tuole station in the upstream, with biases of −13.16 and −12.40 %, respectively; rainfall in Zhangye station simulated by SDM

was overestimated with bias of 14.02 %, and rainfall simulated by DDM was underestimated with bias of −14.60 %; rainfall in Dingxin station simulated by DDM was reproduced better than that by SDM, with biases of −32.75 and −19.34 %, respectively. For a different month, biases of DDM were minor than that of SDM in May, June, and July in Tuole station, and in May, August, and September in Dingxin station, whereas biases of SDM were minor than that of DDM in May, June, and September in Zhangye station. The correlation coefficient of the rainfall in Tuole station between DDM and OBS was 0.43 in July and reached a significance level of 1 %.

Statistical downscaling methods in present studies were implemented in the regions possessing enough meteorological observation stations and good records of rainfall. Thus, SDM had its own shortcoming when applied to the regions lacking of stations, such as the HRB. Therefore, we should think about using satellite-sensing data to assess the capability of SDM and DDM to simulate rainfall in the HRB.

References

Cheng GD, Xiao HL, Xu ZM, et al. (2006) Water issue and its countermeasure in the inland river basin of Northwest China (in Chinese). J Glaciol Geocryol 28:406–413

Dee DP, Uppala SM, Simmons AJ, et al. (2011) The ERA-interim reanalysis: configuration and performance of the data assimilation system. Q J R Meteorol Soc 237:553–597

Denis B, Laprise R, Caya D, et al. (2002) Downscaling ability of one-way nested regional climate models: the big brother experiment. Clim Dyn 18:627–646. doi:10.1007/s00382-001-0201-0

Druyan LM, Fulakeza M, Lonergan P (2002) Dynamical downscaling of seasonal climate predictions over Brazil. J Clim 15:3411–3426

Gao YH, Cheng GD (2008) Several points on mass and energy interaction between land surface and atmosphere in the Heihe River Basin (in Chinese). Adv Earth Sci 23:779–784

Gao YH, Cheng GD, Cui WR, et al. (2006) Coupling of enhanced land surface hydrology with atmospheric mesoscale model and its

implement in the Heihe River Basin (in Chinese). Adv Earth Sci 21: 1283–1292

Gao YH, Cheng GD, Liu W (2007) Setup and validation of the soil texture type distribution data in the Heihe River Basin (in Chinese). Plateau Meteorol 26:958–966

Harding KJ, Snyder PK (2014) Examining future changes in the character of Central U.S. warm-season precipitation using dynamical downscaling. J Geophys Res Atmos 119:13,116–13,136. doi:10.1002/2014JD022575

Houghton JT, Ding Y, Griggs DG, et al. (2001) Climate change: the scientific basis. Cambridge Univ, Cambridge

Kalnay E, Kanamitsu M, Kistler R, Collins W, Deaven D, Gandin L, Iredell M, Saha S, White G, Woollen J, Zhu Y, Leetmaa A, Reynolds B, Chelliah M, Ebisuzaki W, Higgins W, Janowiak J, Mo KC, Ropelewski C, Wang J, Jenne R, Joseph D (1996) The NCEP/NCAR 40-year reanalysis project. Bull Am Meteorol Soc 77:437–471

Lan YC et al. (2005) Change of water resources in mountainous area of Heihe River under global- warming scene (in Chinese). J Desert Res 25:863–868

Lenderink G, Buishand A, van Deursen A (2007) Estimates of future discharges of the river Rhine using two scenario methodologies: direct versus delta approach. Hydrol Earth Syst Sci 11:1145–1159

Liu SH, Jiang HY, Hu F, et al. (2008) A study of surface energy fluxes in Heihe region simulated with a mesosca1e atmospheric model (in Chinese). Chin J Atmos Sci 32:1392–1400

Li Y, Smith I (2008) A statistical downscaling model for Southern Australia Winter Rainfall. J Clim 22:1142–1158

Maraun D, Osborn TJ, Rust HW (2011) The influence of synoptic airflow on UK daily precipitation extremes. Part I: observed spatiotemporal relationships. Clim Dyn 36:261–275

Mearns LO, Bogardei I, Giorgix F, Matyasovszky I, Paleckei M (1999) Comparison of climate change scearios generated from regional climate model experiments and statistical downscaling. J Geophys Res 104:6603–6621

Mehrotra R, Evans JP, Sharma A, Sivakumar B (2014) Evaluation of downscaled daily rainfall hindcasts over Sydney, Australia using statistical and dynamical downscaling approaches. Hydrol Res 45: 226–249

Ruping M, Straus DM (2002) Statistical–dynamical seasonal prediction based on principal component regression of GCM ensemble integrations. Mon Weather Rev 130:2167–2178

Murphy J (1999) An evaluation of statistical and dynamical techniques for downscaling local climate. J Clim 12:2256–2284

Pan XD, Li X, Ran YH, et al. (2012) Impact of underlying surface information on WRF modeling in Heihe River Basin (in Chinese). Plateau Meteorol 31:657–667

Schmidli J et al. (2007) Statistical and dynamical downscaling of precipitation: An evaluation and comparison of scenarios for the European Alps. J Geophys Res 112:D04105

Siegmund J, Bliefernicht J, Laux P, Kunstmann H (2014) Toward a seasonal precipitation prediction system for West Africa: performance of CFSv2 and high–resolution dynamical downscaling. J Geophys Res Atmos 120:7316–7339. doi:10.1002/2014JD022692

Von Storch H, Zorita E, Cubasch U (1993) Downscaling of global climate change estimate to regional scales: an application to Iberian rainfall in wintertime. J Clim 6:1161–1171

Wetterhall F, Bárdossy A, Chen D, Halldin S, Xu CY (2006) Daily precipitation–downscaling techniques in three Chinese regions. Water Resour Res 42:W11423

Wilby RL, Wigley TML (1997) Downscaling general circulation model output: A review of methods and limitations. Prog Phys Geogr 21: 530–548

Wilby RL, Wigley TML (2000) Precipitation predictors for downscaling: observed and general circulation model relationships. Int J Climatol 20:641–661

Xiong Z, Yan XD (2013) Building a high-resolution regional climate model for the Heihe River Basin and simulating precipitation over this region. Chin Sci Bull 58:4670–4678. doi:10.1007/s11434-013-5971-3

Xu JJ et al. (2012) Dynamical downscaling precipitation over southwest Asia: impacts of radiance data assimilation on the forecasts of the WRF-ARW model. Atmos Res 111:90–103

Zhang LJ, Zhao WZ, He ZB, et al. (2008) The characteristics of precipitation and its effects on runoff in a small typical catchment of Qilian Mountain (in Chinese). J Glaciol Geocryol 30:776–782

Zorita E, Hughes JP, et al. (1994) Stochastic characterization of regional circulation patterns for climate model diagnosis and estimation of local precipitation. J Clim 8:1023–1042